Tetrahedron Letters 173 (2025) 155834

Contents lists available at ScienceDirect

Tetrahedron Letters

journal homepage: www.elsevier.com/locate/tetlet

Phosphoric acid-catalyzed regioselective amidation of *para*-quinone methides with acetonitrile

Xiu Liu [a], Hongjun Chen [a,b,*], Chenzhong Jin [a], Longzhi Zhu [c,*], Biquan Xiong [c,d,**]

[a] Key Laboratory of Pesticide Harmless Application in Hunan Higher Education, Hunan Provincial Collaborative Innovation Center for Field Weeds Control, Hunan University of Humanities, Science and Technology, Loudi 417000, PR China
[b] Hunan Provincial Key Laboratory of Fine Ceramics and Powder Materials, School of Materials and Environmental Engineering, Hunan University of Humanities, Science and Technology, Loudi 417000, PR China
[c] Department of Chemistry and Chemical Engineering, Hunan Institute of Science and Technology, Yueyang 414006, PR China
[d] Department of Applied Biology and Chemical Technology, The Hong Kong Polytechnic University, Hung Hom, PR China

ARTICLE INFO

Keywords:
Amidation
Acetonitrile
Ritter-type amidation
para-Quinone methides

ABSTRACT

An efficient and atom-economical phosphoric acid-catalyzed amidation of *para*-quinone methides (*p*-QMs) with acetonitrile has been developed under mild conditions. Water serves as the sole source of both hydrogen and oxygen atoms, enabling 100 % atom economy in amide bond formation. The reaction exhibits excellent generality across a broad spectrum of electronically and sterically diverse *p*-QMs, facilitating efficient and highly regioselective synthesis of synthetically valuable *N*-diarylmethyl-substituted acetamides in good to excellent yields. Step-by-step control experiments and competitive deuterium-labeling KIE studies elucidated the reaction pathway and led to a plausible mechanism based on cumulative experimental evidences.

Introduction

The amide bond is one of the most fundamental chemical motifs prevalent in nature, forming the structural backbone of essential biological peptides and proteins [1–4]. It is also ubiquitous in diverse compounds, including natural products and pharmaceuticals [5]. In addition, organic amides serve as pivotal synthetic intermediates, finding extensive application in the development of pharmacologically active agents, polymer precursors, optoelectronic materials, flame retardants, and pesticides [6,7]. Among these compounds, *N*-diarylmethyl-substituted amides merit particular highlighting due to their distinctive structural attributes and resultant properties, underpinning their widespread utility in life sciences and pharmaceutical research (Scheme 1) [8–11]. This significance stems from the bulky hydrophobic diarylmethyl moiety, which enhances metabolic stability by shielding the amide bond from enzymatic hydrolysis. Concurrently, this group strengthens target binding affinity and modulates biological activity through mechanisms such as π-π stacking interactions and hydrophobic cavity occupancy. Notably, when the two aryl substituents are dissimilar, a chiral center is generated. This chirality governs stereoselective biological activity, as exemplified by the enantiomeric divergence observed in carfilzomib, thereby providing a critical strategic avenue for precision drug design. Consequently, given the broad applicability of *N*-diarylmethyl-substituted amides across multiple disciplines, the development of efficient and cost-effective methodologies for their synthesis holds substantial theoretical and practical significance [12–17].

The direct catalytic amidation of carboxylic acids with organic amines, facilitated by catalysts without employing activating reagents, represents an ideal green pathway for amide synthesis by circumventing drawbacks associated with activating agents [18]. However, these methods generally necessitate prolonged reaction times and elevated temperatures (>160 °C), exhibit limited substrate scope, and consequently have not gained widespread adoption. Conventional amide synthesis relies on the condensation of carboxylic acids or more reactive derivatives (*e.g.,* acyl chlorides, anhydrides, esters) with amines or ammonia at appropriate temperatures [14]. This approach suffers from low atom economy, difficult separation procedures, and the generation of environmentally detrimental byproducts. Beyond conventional methods, reported synthetic strategies for amides primarily include: (1) carbonyl insertion reactions using haloalkanes, amines, and carbon

* Corresponding author at: Key Laboratory of Pesticide Harmless Application in Hunan Higher Education, Hunan Provincial Collaborative Innovation Center for Field Weeds Control, Hunan University of Humanities, Science and Technology, Loudi 417000, PR China.
** Corresponding author at: Department of Chemistry and Chemical Engineering, Hunan Institute of Science and Technology, Yueyang 414006, PR China.
E-mail addresses: hongjunchen@hnu.edu.cn (H. Chen), zhulongzhi@hnu.edu.cn (L. Zhu), xiongbiquan@126.com (B. Xiong).

https://doi.org/10.1016/j.tetlet.2025.155834
Received 14 August 2025; Received in revised form 17 September 2025; Accepted 19 September 2025
Available online 20 September 2025

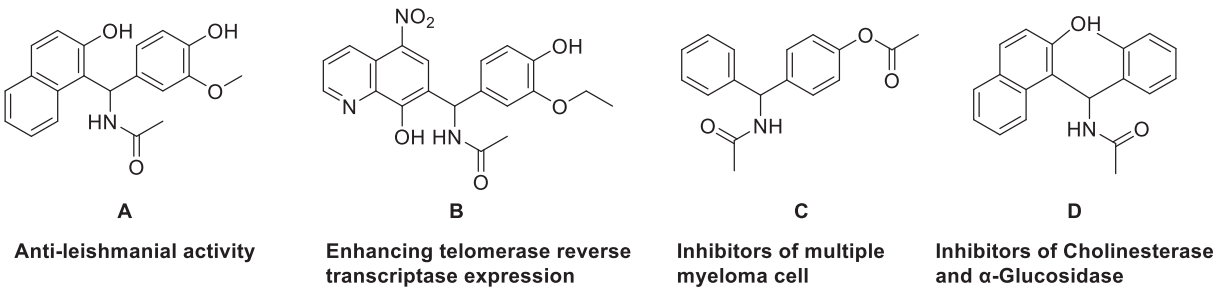

Scheme 1. Important *N*-diarylmethyl-substituted amides.

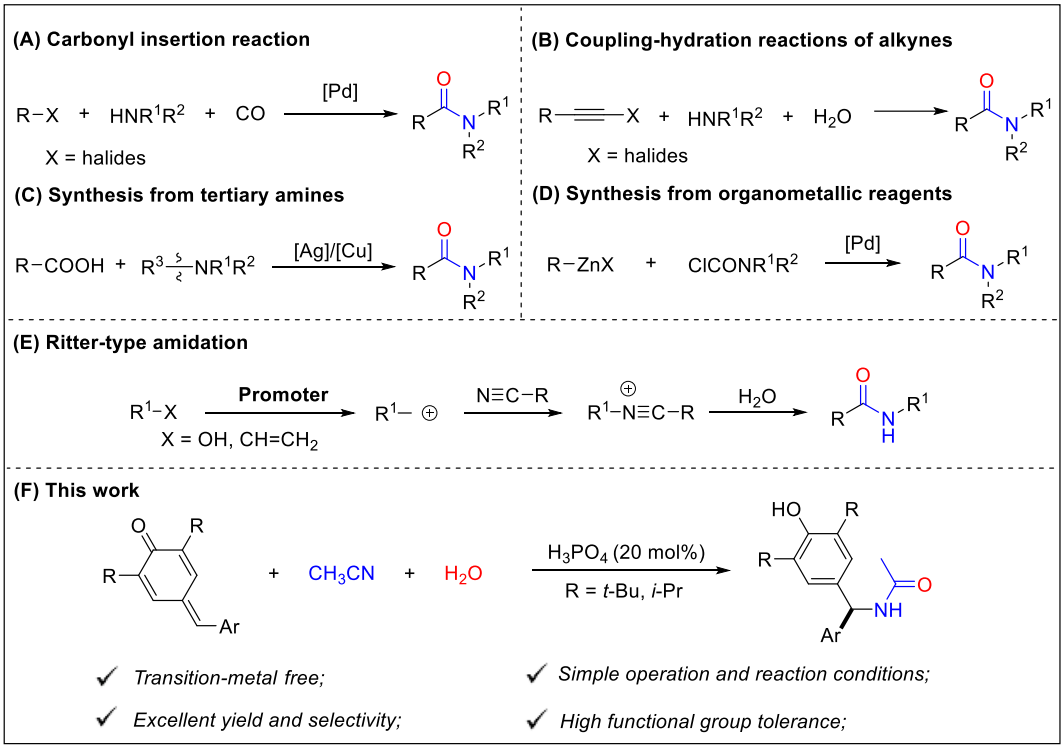

Scheme 2. Methods for the synthesis of amides.

monoxide or employing benzyl-substituted arenes, amines, and carbon monoxide (Scheme 2A) [19,20]; (2) coupling-hydration reactions of alkynyl halides with primary amines and water (Scheme 2B) [21]; (3) transition-metal-catalyzed coupling of carboxylic acids with tertiary amines *via* C—N bond cleavage (Scheme 2C) [22,23]; and (4) three-component cross-coupling reactions involving organometallic reagents (*e.g.*, organozinc, organomagnesium), and carbamoyl chlorides (Scheme 2D) [24]. Recently, Ritter-type amidation employing alcohols [25–28], olefins [29], or other active carbon centers [30–35] has also been developed for the synthesis of amides (Scheme 2E). Nevertheless, these methods typically require precious metal catalysts and air-sensitive reagents. Furthermore, they are often plagued by drawbacks such as cumbersome procedures, expensive and difficult-to-recycle catalysts, harsh reaction conditions, limited substrate applicability, modest yields, and significant environmental pollution. Additionally, studies specifically focused on synthesizing diarylmethane-substituted amides remain scarce.

para-Quinone methides (*p*-QMs), categorized as a distinct class of electron-deficient olefins owing to their unique electronic properties, serve as pivotal building blocks in organic synthesis [36–42]. They readily participate in 1,6-conjugate addition/arylation reactions, facilitating the construction of diverse bonds—including C—C [43–46], C—O [47], C—N [48–52], C—S [53,54], C—Si [55], and C—P [56,57] linkages. This reactivity underpins their widespread application for synthesizing functionalized aryl methane derivatives. Motivated by our group's sustained research focus on *p*-QMs [57–63], we devised a general and environmentally benign protocol for synthesizing diarylmethane-substituted amides (Scheme 2F). This transformation operates under mild conditions, obviating the requirement for transition metals. Significantly, it incorporates a novel design utilizing water as a combined hydrogen and oxygen source, thereby establishing a new strategy for the efficient utilization of acetonitrile.

Results and discussion

The unique electron-deficient olefin character of *p*-QMs enables their ready formation of a key carbocation intermediate at the C7 position under protonic acid catalysis. This property prompted the proposal that introducing acetonitrile as a nucleophilic acceptor simultaneously with carbocation generation, along with water serving as the oxygen and hydrogen source, could facilitate *in-situ* activation of the nitrile group, thereby enabling an amidation reaction with *p*-QMs. To validate this hypothesis, exploratory reaction was conducted using 4-benzylidene-2,6-di-*tert*-butylcyclohexa-2,5-dienone (**1a**) and acetonitrile (**2a**) as

Table 1
Optimization of the reaction conditions.[a]

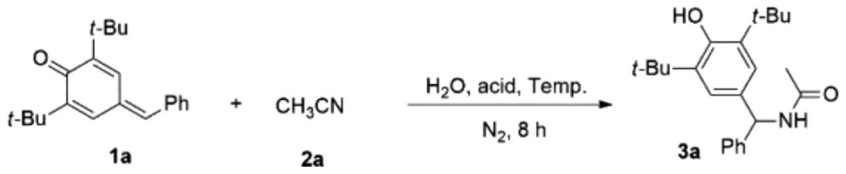

Entry	Solvent	Acid (Mol%)	H_2O (eq.)	Temp. (°C)	Yield[b]
1	CH_3CN	H_3PO_4 (10)	2.0	100	78 %
2	CH_3CN	HCl (10)	2.0	100	76 %
3	CH_3CN	H_2SO_4 (10)	2.0	100	73 %
4	CH_3CN	CF_3COOH (10)	2.0	100	54 %
5	CH_3CN	TfOH (10)	2.0	100	56 %
6	CH_3CN	TsOH (10)	2.0	100	52 %
7	CH_3CN	H_3PO_4 (0)	2.0	100	N.D[c]
8	CH_3CN	H_3PO_4 (15)	2.0	100	81 %
9	CH_3CN	H_3PO_4 (20)	2.0	100	86 %
10	CH_3CN	H_3PO_4 (25)	2.0	100	85 %
11	CH_3CN	H_3PO_4 (20)	2.0	25	N.D[c]
12	CH_3CN	H_3PO_4 (20)	2.0	40	43 %
13	CH_3CN	H_3PO_4 (20)	2.0	60	54 %
14	**CH_3CN**	**H_3PO_4 (20)**	**2.0**	80	**96 %**
15	Toluene	H_3PO_4 (20)	2.0	80	N.D[c,d]
16	CH_2Cl_2	H_3PO_4 (20)	2.0	80	trace[d]
17	Acetone	H_3PO_4 (20)	2.0	80	N.D[c,d]
18	THF	H_3PO_4 (20)	2.0	80	< 10 %[d]
19	DMSO	H_3PO_4 (20)	2.0	80	N.D[c,d]
20	1,4-Dioxane	H_3PO_4 (20)	2.0	80	trace[d]
21	DMF	H_3PO_4 (20)	2.0	80	N.D[c,d]
22	CH_3CN	H_3PO_4 (20)	0	80	N.D[c]
23	CH_3CN	H_3PO_4 (20)	1.0	80	73 %
24	CH_3CN	H_3PO_4 (20)	3.0	80	93 %

[a] Reactions were carried out with 4-benzylidene-2,6-di-*tert*-butylcyclohexa-2,5-dienone (**1a**, 0.2 mmol), acetonitrile (**2a**, 1.0 mL), Acid (x mol%), H_2O (x eq), under a N_2 atmosphere stirred for 8 h at x °C.
[b] Yield was determined by GC analysis, using dodecane as the internal standard.
[c] N.D. = Not detected.
[d] for entries 15–21, 1.0 mmol of CH_3CN was added.

model substrates. Under catalysis by phosphoric acid (10 mol%), using an excess of acetonitrile (1.0 mL) serving dual roles as both reactant and solvent, the reaction proceeded at 100 °C under a nitrogen atmosphere for 8 h. Analysis by GC, GC–MS, and NMR confirmed the successful synthesis of the target product, *N*-((3,5-di-*tert*-butyl-4-hydroxyphenyl)(phenyl)methyl)acetamide (**3a**), with a yield of 78 %. The preliminary results confirmed the feasibility of the reaction pathway, prompting a systematic investigation into the influence of key reaction parameters.

The catalytic efficacy of various protonic acid catalysts (*e.g.*, HCl, H_2SO_4, CF_3COOH, TfOH, TsOH) was further evaluated at an equimolar loading (10 mol%) (Table 1, entries 2–6). The results indicated that phosphoric acid exhibited the optimal catalytic activity. Subsequently, optimization of the phosphoric acid loading was focused on (Table 1, entries 7–10). Control experiments revealed no detectable target product in the absence of phosphoric acid. As the catalyst loading increased from 5 mol% to 20 mol%, the yield of **3a** significantly improved, reaching a maximum of 86 % at 20 mol%. Further increasing the loading to 25 mol% showed no yield enhancement, thus establishing 20 mol% as the optimal catalyst amount. Reaction temperature was also a critical factor (Table 1, entries 11–14). No reaction occurred at room temperature; product **3a** formation commenced upon heating to 40 °C. The yield continuously increased with rising temperature, achieving an optimal yield of 96 % at 80 °C; however, the yield slightly decreased to 78 % when the temperature was elevated to 100 °C. Furthermore, the solvent effect and the role of water were investigated. Maintaining a fixed amount of acetonitrile (1.0 mmol, 5.0 equiv.) as the reactant, the influence of various solvents (*e.g.*, toluene, dichloromethane, acetone, THF, DMSO, 1,4-dioxane, DMF) on the transformation was examined (Table 1, entries 15–21). However, effective formation of **3a** was not observed in any of these solvent systems, clearly indicating that acetonitrile acting as the solvent is crucial for this reaction. Finally, the role of water as the oxygen and hydrogen source and its optimal amount were explored (Table 1, entries 22–24). The reaction was completely suppressed under anhydrous conditions. The yield of **3a** progressively increased as the water equivalents were raised (0.5 to 2.0 equiv); however, further increasing the water amount to 3.0 equiv. did not result in additional yield improvement. Therefore, the optimized conditions for this transformation were established as follows: *p*-QMs (0.2 mmol), acetonitrile (1.0 mL, serving as solvent and substrate), phosphoric acid (20 mol%), water (2.0 equiv.), at 80 °C for 8 h.

As detailed in Table 2, to systematically evaluate the influence of diverse substituents (incorporating both electronic and steric effects) on the adaptability of *p*-QMs in amidation reactions, we investigated the reactions of a series of *p*-QMs bearing various functional groups with acetonitrile under optimized reaction conditions. The results clearly demonstrate that, under phosphoric acid catalysis, the substrates possessing electron-donating groups (EDGs) on the aryl ring generally exhibit high reactivity, with substrates containing EDGs such as 4-Et (**1b**), 4-*t*-Bu (**1c**), 4-O-*i*Pr (**1d**), and 3-OMe (**1f**) being efficiently converted to the corresponding amide products in excellent yields (82–91 %); this enhanced reactivity is attributed to the ability of EDGs to stabilize key electrophilic intermediates (*e.g.*, iminium ions or analogous species) through their positive electronic effect, thereby facilitating the 1,6-conjugate addition step. Notably, the reactivity profile diverges when EDGs are located at the *ortho*-position of the phenyl ring, as exemplified by substrates 2-OMe (**1g**), 2-Me (**1h**), 2-OEt (**1i**), and 2-OBn (**1j**), where although electronically favorable, the *ortho*-placement introduces significant steric encumbrance that, while not precluding

Table 2
Substrate scope of *p*-QMs.[a,b]

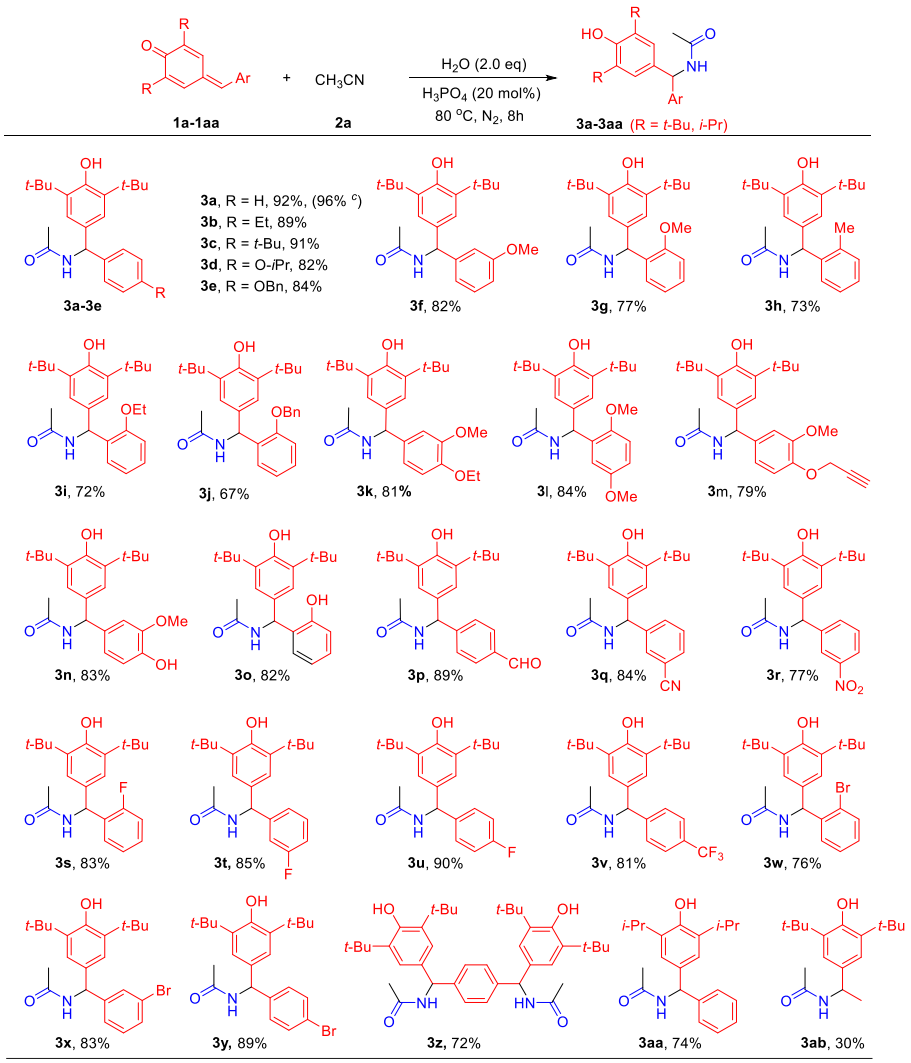

[a] Reaction conditions: *p*-QMs compounds (**1a-1aa**, 0.2 mmol), acetonitrile (**2a**, 1.0 mL), H_3PO_4 (20 mol%), H_2O (2.0 eq), N_2, 80 °C, 8 h. [b] Isolated yields. [c] GC yield.

reaction, resulting in the target amides being obtained in moderate yields (67–77 %); a discernible decrease in yield was observed for these *ortho*-substituted analogues compared to their *para*- or *meta*-substituted counterparts, highlighting the critical role of steric factors in this reaction system as *ortho*-substituents likely impose physical constraints that impede access to the reaction center, compromise intermediate conformational stability, or hinder subsequent transformation steps, partially counteracting the beneficial electronic contribution. Furthermore, a series of polysubstituted *p*-QMs bearing various substituents on the phenyl ring—including including 4-ethoxy-3-methoxy (**1k**), 2,5-dimethoxy (**1l**), 3-methoxy-4-(prop-2-yn-1-yloxy) (**1m**), and 4-hydroxy-3-methoxy (**1n**)—were evaluated. Although these functional groups introduce both electronic and steric influences, the results suggest that steric effects may not have prevailed under these conditions, thus enabling the formation of the corresponding amide products in good yields (79–84 %). Crucially, the amidation reaction demonstrated excellent compatibility with specialized substrates containing reactive functional groups, such as -OH (**1o**), -CHO (**1p**), affording the target amides **3o** and **3p** in 82 % and 89 % yield, respectively. Importantly, the reactive functional groups remained largely intact throughout the process. Their preservation in the products **3o** and **3p** offers considerable synthetic utility, as these sites can be leveraged for selective post-functionalization *via* cross-coupling, condensation, or cyclization reactions. This capability could facilitate the modular synthesis of structurally diverse small molecules—potentially with bioactivity—based on the core amide products.

On the other hand, *p*-QMs bearing electron-withdrawing substituents on the phenyl ring—including 3-CN (**1q**), 3-NO_2 (**1r**), 2-F (**1s**), 3-F (**1t**), 4-F (**1u**), 4-CF_3 (**1v**), 2-Br (**1w**), 3-Br (**1x**), and 4-Br (**1y**)—demonstrated positive reactivity in the amidation reaction with acetonitrile. The corresponding products **3q-3y** were isolated in 76–90 % yields. Notably, substrates with electron-withdrawing groups afforded moderately lower yields in this transformation compared to their electron-donating counterparts. This diminished efficiency might be attributed to reduced electron density at the phenyl ring imposed by electron-withdrawing substituents, which attenuates the electrophilic character of the pivotal C7 alkenyl moiety in *p*-QMs. Furthermore, steric perturbations induced by *ortho*-substituents (*e.g.*, **1s**, **1w**) constitute a non-negligible factor in evaluating electronic effects. To further probe the versatility of this system toward multifunctional substrates, 4,4′-(1,4-phenylenebis(methanylylidene))bis(2,6-di-*tert*-butylcyclohexa-2,5-dienone) (**1z**) was employed. This *bis*-*p*-QM scaffold presents two susceptible alkenyl sites. Under optimized conditions, difunctionalization proceeded efficiently, furnishing the bis-amidated product *N*,*N*′-(1,4-

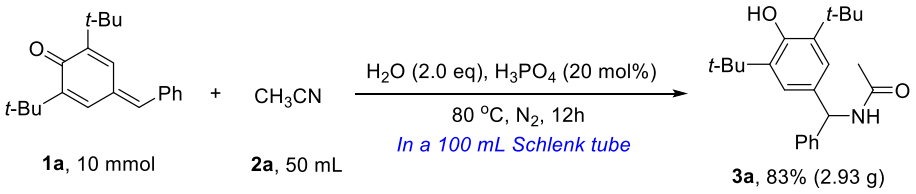

Scheme 3. Gram-scale synthesis of **3a**.

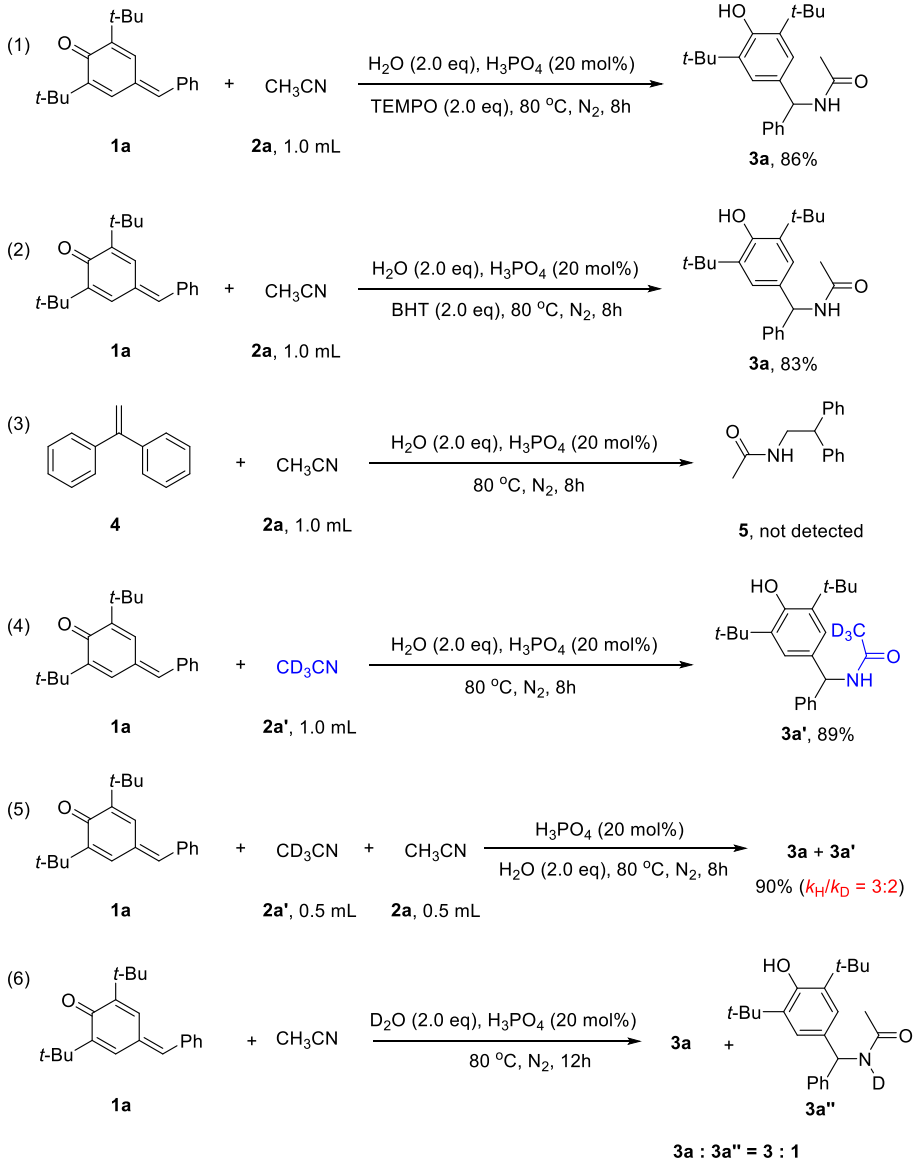

Scheme 4. Step-by-step control experiments.

phenylenebis((3,5-di-*tert*-butyl-4-hydroxyphenyl)methylene))diacetamide (**3z**) in 72 % yield. This outcome indicates that the phosphoric acid-catalyzed amidation protocol may be a useful strategy for the modular functionalization of polyreactive architectures. Moreover, to evaluate structural diversity, we investigated both the isopropyl-variant (**1aa**) and the methyl-substituted *p*-QM (**1ab**). Compound **1aa**, bearing less sterically demanding and electron-donating isopropyl groups, exhibited reduced stability relative to the *tert*-butyl analogues, affording product **3aa** in 74 % yield likely due to competing decomposition or side reactions. Under the same conditions, the more reactive methyl-substituted substrate **1ab** gave the desired product **3ab** in 30 % yield, reflecting diminished selectivity but still demonstrating applicability across diverse *p*-QM scaffolds.

To assess the practical applicability of this amidation transformation, a gram-scale synthesis was performed (Scheme 3). Using substrate **1a** (10 mmol) in acetonitrile (50 mL, acting as both reactant and solvent), the reaction was carried out in a 100 mL Schlenk tube under optimized conditions. Considering potential variations in mass transfer efficiency, mixing dynamics, and thermodynamic profiles during scale-up, the reaction time was extended from 8 h (standard conditions) to 12 h. Upon completion, the target product **3a** was isolated through simple column chromatography, affording 2.93 g in 83 % isolated yield.

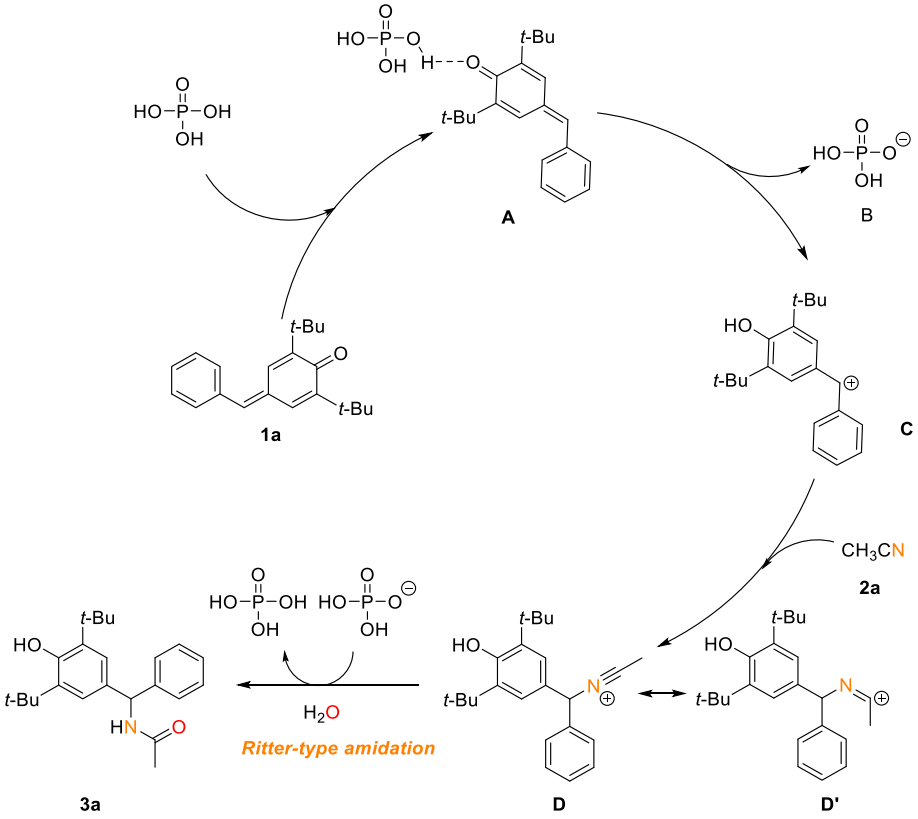

Scheme 5. A plausible mechanism.

To elucidate the possible mechanism of this reaction, a series of stepwise control experiments were performed. Initially, based on the optimized reaction conditions and using the model reaction as a benchmark, radical scavengers (such as TEMPO and BHT) were separately introduced into the reaction system to investigate potential involvement of a radical pathway. Analysis by GC and GC–MS upon reaction completion revealed that the target product **3a** was still obtained in significant yields (86 % and 83 %, respectively, Scheme 4, entries 1–2) in the presence of TEMPO or BHT, with no radical-trapped adducts detected. Notably, the slight decrease in yield compared to the control experiment without scavengers is more likely attributable to the physical effects of the inhibitors themselves (*e.g.*, dilution or competitive adsorption) rather than inhibition of a radical pathway. This key observation indicates that a radical intermediate process is unlikely for this amidation reaction. Given that *para*-quinone methides can be regarded as a class of electron-deficient alkenes with specific characteristics, we further examined the necessity of **1a** in this transformation. When structurally analogous 1,1-diphenylethylene (**4**) was employed in place of **1a**, the target product *N*-(2,2-diphenylethyl)acetamide (**5**) was completely undetected, and the starting material 1,1-diphenylethylene remained largely unreacted (Scheme 4, entry 3). This result strongly supports the indispensability of the *p*-QMs structure in the reaction, suggesting that its specific electronic or steric properties may be crucial for reactivity. Furthermore, solvent kinetic isotope effect (KIE) experiments were conducted accordingly. When acetonitrile (CH_3CN) was completely replaced by deuterated acetonitrile (CD_3CN) as the solvent, the deuterated target product **3a'** was obtained in 89 % isolated yield. To quantitatively assess the extent of solvent participation, a competitive kinetic experiment was performed: equal volumes (0.5 mL each) of CH_3CN and CD_3CN were added simultaneously to the standard reaction mixture. After completion, the target product was isolated and purified, and its H/D ratio was analyzed by ^1H NMR, yielding a kinetic isotope effect (KIE) value of $k_H/k_D = 1.5$ (corresponding to a 3:2 ratio) (Scheme 4, entries 4–5). Furthermore, when the reaction was carried out using deuterated water (D_2O) in place of regular water, a mixture of the original product **3a** and its deuterated analog **3a"** was isolated (Scheme 4, entry 6). The relatively low deuterium incorporation (approximately 25 %) is likely attributable to H/D exchange with protic solvents or ambient moisture during the reaction or workup process.

Based on the above control experiments and literature reports [64,65], we propose a plausible reaction mechanism as shown in Scheme 5. Initially, phosphoric acid (H_3PO_4) attacks the C═O group of *p*-QMs (**1a**) to produce intermediate **A** [66]. Subsequently, *via* hydrogen bonding, carbocation intermediate **C** and anion $H_2PO_4^-$ (**B**) are formed. The lone pair electrons on the nitrogen atom of acetonitrile (**2a**) then attack the carbocation center of intermediate **C** to form intermediate **D**, which isomerizes to intermediate **D′**. Finally, the lone pair electrons on the oxygen atom of water attack **D′**, undergoing Ritter-type amidation to afford the target product **3a**. Concurrently, anion **B** captures the proton released during the Ritter-type amidation process, regenerating the phosphoric acid catalyst to participate in the next catalytic cycle.

Conclusions

In summary, we successfully established a novel, highly efficient, and atom-economical strategy for the phosphoric acid-catalyzed amidation of *p*-QMs with acetonitrile under mild conditions. The core innovation lay in the ingenious utilization of water molecules as the sole source of both hydrogen and oxygen atoms, thereby achieving 100 % atom economy in the amide bond formation. The reaction exhibited excellent substrate generality, accommodating *p*-QM substrates with diverse electronic properties and significant steric variations, and efficiently provided synthetically valuable *N*-diarylmethylacetamides with high stereoselectivity in good to excellent yields. Systematic mechanistic investigations, including stepwise control experiments and competitive deuterium kinetic isotope effect (KIE) studies, elucidated the reaction

pathway, and a plausible mechanism was proposed based on the cumulative experimental evidence. This protocol featured straightforward operation, mild conditions, environmental benignity, high efficiency, perfect atom utilization, and broad applicability, collectively establishing the phosphoric acid-catalyzed process as a valuable new strategy for green synthesis.

Experimental section

General Considerations: All solvents used in the reactions were freshly distilled. The other reagents were recrystallized or distilled as necessary. All reactions were performed under an atmosphere of dry nitrogen unless specified otherwise. ^{1}H (400 MHz) and ^{13}C (101 MHz) were recorded on a 400 MHz spectrometer in $CDCl_3$ or DMSO-d_6. ^{1}H NMR chemical shifts were reported using TMS as the internal standard while ^{13}C NMR chemical shifts were reported relative to $CDCl_3$. The electron ionization method was used for HRMS measurements, and the mass analyzer type was double-focusing.

General procedure: A mixture of *para*-quinone methides (*p*-QMs) (0.2 mmol), CH_3CN (1.0 mL), H_3PO_4 (20 mol%), H_2O (2.0 eq), under a N_2 atmosphere stirred for 8 h at 80 °C. Upon completion of the reaction, the mixture was concentrated under vacuum. Removal of the solvent under a reduced pressure gave the crude product; pure product was obtained by passing the crude product through a short silica gel column using hexane/EtOAc (80:1–20:1) as eluent.

Supporting Information Available: Copies of ^{1}H and ^{13}C NMR spectra and the corresponding NMR characterization data.

CRediT authorship contribution statement

Xiu Liu: Investigation, Data curation. **Hongjun Chen:** Supervision, Investigation, Data curation. **Chenzhong Jin:** Visualization, Data curation, Conceptualization. **Longzhi Zhu:** Writing – original draft, Visualization. **Biquan Xiong:** Writing – review & editing, Supervision.

Declaration of competing interest

The authors declare that they have no known competing financial interests or personal relationships that could have appeared to influence the work reported in this paper.

Acknowledgments

This work is supported by the Natural Science Foundation of Hunan Province (Nos. 2023JJ50082, 2024JJ7252), Scientific Research Fund of Hunan Provincial Education Department (Nos. 22A0614), Pesticide Harmless Application of Science and Technology Innovative Team in Higher Education Institutions of Hunan Province (2023), the Double First-Class Discipline Construction Program of Hunan Province, and Hunan Provincial College Student Innovation and Entrepreneurship Training Program.

Appendix A. Supplementary data

Supplementary data to this article can be found online at https://doi.org/10.1016/j.tetlet.2025.155834.

Data availability

Data will be made available on request.

References

[1] A. Garg, T. Thakral, R. Dhiman, A. Bhalla, Tetrahedron Lett. 153 (2024) 155383.
[2] J. Magano, Org. Process Res. Dev. 26 (2022) 1562.
[3] A. Bedini, G. Spadoni, G. Gatti, S. Lucarini, G. Tarzia, S. Rivara, S. Lorenzi, A. Lodola, M. Mor, V. Lucini, M. Pannacci, F. Scaglione, J. Med. Chem. 49 (2006) 7393.
[4] C.A.G.N. Montalbetti, V. Falque, Tetrahedron 61 (2005) 10827.
[5] D.G. Brown, J. Boström, J. Med. Chem. 59 (2015) 4443.
[6] P. Hu, Y. Ben-David, D. Milstein, Angew. Chem. Int. Ed. 55 (2015) 1061.
[7] T. Lu, Z. Lu, Z.-X. Ma, Y. Zhang, R.P. Hsung, Chem. Rev. 113 (2013) 4862.
[8] N.R. Rode, A.A. Tantray, A.V. Shelar, R.H. Patil, S.S. Terdale, Res. Chem. Intermed. 48 (2022) 2391.
[9] K. Boudebbous, H. Boulebd, C. Bensouici, D. Harakat, R. Boulcina, A. Debache, Chemistryselect 5 (2020) 5515.
[10] T. Misawa, K. Dodo, M. Ishikawa, Y. Hashimoto, M. Sagawa, M. Kizaki, H. Aoyama, Bioorg. Med. Chem. 23 (2015) 2241.
[11] H. William, Lancer K. Brown, N.V. Sparks, Laura A. Briggs, N.V. Reno, Federico C. A. Gaeta, Mountain View, CA; Hamid Mohammadpour, Reno, NV; Mieczyslaw A. Piatyszek, Gainesville, FL In 8-Hydroxy quinoline derivatives for enhancing telomerase reverse transcriptase (TERT) expression, United State, 2023.
[12] X. Wang, Nat. Catal. 2 (2019) 98.
[13] V.R. Pattabiraman, J.W. Bode, Nature 480 (2011) 471.
[14] H. Lundberg, F. Tinnis, N. Selander, H. Adolfsson, Chem. Soc. Rev. 43 (2014) 2714.
[15] X. Deng, G. Zhou, J. Tian, R. Srinivasan, Angew. Chem. Int. Ed. 60 (2020) 7024.
[16] A.S. Santos, A.M.S. Silva, M.M.B. Marques, Eur. J. Org. Chem. 2020 (2020) 2501.
[17] S. Liu, Z. Zhang, Y. Yang, J. Huang, Chin. J. Org. Chem. 44 (2024) 409.
[18] P.A. Grieco, D.S. Clark, G.P. Withers, J. Org. Chem. 44 (1979) 2945.
[19] L. Troisi, C. Granito, F. Rosato, V. Videtta, Tetrahedron Lett. 51 (2010) 371.
[20] P. Xie, C. Xia, H. Huang, Org. Lett. 15 (2013) 3370.
[21] Z.-W. Chen, H.-F. Jiang, X.-Y. Pan, Z.-J. He, Tetrahedron 67 (2011) 5920.
[22] B. Xiong, L. Zhu, X. Feng, J. Lei, T. Chen, Y. Zhou, L.-B. Han, C.-T. Au, S.-F. Yin, Eur. J. Org. Chem. 2014 (2014) 4244.
[23] X. Zhang, W. Yang, L. Wang, Org. Biomol. Chem. 11 (2013) 3649.
[24] R.D. Rieke, S.-H. Kim, Tetrahedron Lett. 53 (2012) 3478.
[25] K.V. Katkar, P.S. Chaudhari, K.G. Akamanchi, Green Chem. 13 (2011) 835.
[26] S.H. Doan, M.A. Hussein, T.V. Nguyen, Chem. Commun. 57 (2021) 8901.
[27] E. Soliman, H. Baek, N. Mase, Y.M.A. Yamada, J. Org. Chem. 90 (2025) 1447.
[28] L. Zhu, F. Guo, W. Luo, S. Xie, T. Zhu, Z. Liao, B. Xiong, Y. Liu, K. Tang, R. Qiu, Green Chem. 27 (2025) 11125.
[29] S. Liu, M. Klussmann, Org. Chem. Front. 8 (2021) 2932.
[30] Q. Michaudel, D. Thevenet, P.S. Baran, J. Am. Chem. Soc. 134 (2012) 2547.
[31] L. Zhang, Y. Fu, Y. Shen, C. Liu, M. Sun, R. Cheng, W. Zhu, X. Qian, Y. Ma, J. Ye, Nat. Commun. 13 (2022) 4138.
[32] T. Shen, T.H. Lambert, J. Am. Chem. Soc. 143 (2021) 8597.
[33] L. Bao, B.-B. Zhang, Z.-X. Wang, X.-Y. Chen, Org. Chem. Front. 10 (2023) 1375.
[34] R. Narobe, K. Murugesan, C. Haag, T.E. Schirmer, B. König, Chem. Commun. 58 (2022) 8778.
[35] M.-E. Chen, S.-Z. Tang, Y.-H. Hu, Q.-T. Li, Z.-Y. Gan, J.-W. Lv, F.-M. Zhang, CCS Chem. 4 (2022) 3378.
[36] J.-Y. Wang, W.-J. Hao, S.-J. Tu, B. Jiang, Org. Chem. Front. 7 (2020) 1743.
[37] C.G.S. Lima, F.P. Pauli, D.C.S. Costa, A.S.D. Souza, L.S.M. Forezi, V.F. Ferreira, F.D. C.D. Silva, Eur. J. Org. Chem. (2020) 2650.
[38] Z.-P. Zhang, N. Dong, X. Li, Chem. Commun. 53 (2017) 1301.
[39] P.-Z. Zi, X.-B. Liu, Q.-H. Zhao, M. He, Y. Huang, Green Synth. Catal. 5 (2024) 68.
[40] S. Li, Y. Liu, B. Huang, T. Zhou, H. Tao, Y. Xiao, L. Liu, J. Zhang, ACS Catal. 7 (2017) 2805.
[41] H. Qinggao, L. Xianping, C. Liyong, C. Renfeng, Y. Sitong, Z. Longzhi, X. Biquan, Curr. Org. Chem. 29 (2025) 1221.
[42] X. Liu, Y. Ren, L. Zhu, T. Li, W. Xu, Y. Liu, K.-W. Tang, B. Xiong, Tetrahedron 148 (2023) 133655.
[43] S. Santra, A. Porey, B. Jana, J. Guin, Chem. Sci. 9 (2018) 6446.
[44] Z. Liu, H. Xu, T. Yao, J. Zhang, L. Liu, Org. Lett. 21 (2019) 7539.
[45] A.A. Fadeev, M. Kotora, Org. Biomol. Chem. 21 (2023) 6174.
[46] T.-S. Zhang, J. Li, H. Sun, S. Liu, J. Li, Y. Chen, W.-J. Hao, B. Jiang, Tetrahedron (2023) 147.
[47] P.-Q. Ren, Y.-F. Li, S.-Y. Wang, Y.-S. Luo, M. Liu, R.-H. Li, Y.-Y. Zeng, ACS Omega 10 (2025) 3044.
[48] L. Fan, L. Zhu, W. Shang, M. Yin, B. Xiong, W. Xie, F. Cao, Y. Liu, Y. Chen, R. Qiu, Adv. Synth. Catal. 366 (2024) 2101.
[49] R. Venkatesh, K. Gurukkalot, V. Rajendran, J. Kandasamy, Org. Biomol. Chem. 23 (2025) 383.
[50] R. Dash, S.K. Hota, S. Murarka, Synthesis 56 (2023) 677.
[51] S. Guin, H.K. Saha, A.K. Patel, S.K. Gudimella, S. Biswas, S. Samanta, Tetrahedron (2020) 76.
[52] K. Chen, W.-J. Hao, S.-J. Tu, B. Jiang, Green Chem. 21 (2019) 675.
[53] Y. Zhong, G. Li, D. Zhang, Y. Xie, L. Hao, Z. Cai, X. Wang, Eur. J. Org. Chem. 27 (2024) e202400130.
[54] Y.-J. Fan, L. Zhou, S. Li, Org. Chem. Front. 2018 (1820) 5.
[55] C. Luo, W.-H. Lu, G.-Q. Wang, Z.-B. Zhang, H.-Q. Li, P. Han, D. Yang, L.-H. Jing, C. Wang, J. Org. Chem. 87 (2022) 3567.
[56] N. Molleti, J.Y. Kang, Org. Lett. 19 (2017) 958.
[57] S. Xu, J. Xie, Y. Liu, W. Xu, K.-W. Tang, B. Xiong, W.-Y. Wong, J. Org. Chem. 86 (2021) 14983.
[58] M. Yuan, Z. Li, W. Xu, B. Xiong, Y. Liu, M. Liu, K.W. Tang, L. Zhu, Chin. J. Chem. 43 (2025) 191.
[59] M. Yuan, Z. Li, W. Shang, B. Xiong, W. Xu, L. Zhu, Y. Liu, K.-W. Tang, W.-Y. Wong, J. Org. Chem. 89 (2024) 16663.
[60] L. Zhu, Y. Ren, X. Liu, S. Xu, T. Li, W. Xu, Z. Li, Y. Liu, B. Xiong, Chem. Asian J. 18 (2023) e202300792.

[61] W. Shang, L. Zhu, Z. Li, W. Xu, B. Xiong, Y. Liu, K.-W. Tang, P.-C. Qian, S.-F. Yin, W.-Y. Wong, J. Org. Chem. 88 (2023) 16196.
[62] B. Xiong, S. Xu, W. Xu, Y. Liu, L. Zhang, K.-W. Tang, S.-F. Yin, W.-Y. Wong, Org. Chem. Front. 9 (2022) 3807.
[63] B. Xiong, S. Xu, Y. Liu, K.W. Tang, W.Y. Wong, J. Org. Chem. 86 (2021) 1516.
[64] Y.-C. Hu, Y. Li, D.-W. Ji, H. Liu, H. Zheng, G. Zhang, Q.-A. Chen, Chin. J. Catal. 42 (2021) 1593.
[65] X. Mo, D.G. Hall, J. Am. Chem. Soc. 138 (2016) 10762.
[66] B. Xiong, L. Si, Y. Liu, W. Xu, T. Jiang, F. Cao, K.W. Tang, W.Y. Wong, Chem. Asian J. 17 (2022) e202200042.